**Table 1　Baseline patient characteristics**

| | Total | CAD(−) | CAD(+) |
|---|---|---|---|
| n | 38 | 19 | 19 |
| Age (years) | 65 ± 12 | 68 ± 15 | 63 ± 9 |
| Sex (% male) | 64 | 60 | 72 |
| Smoking habit (%) | 25 | 15 | 35 |
| Duration of CHF (years) | 3.2 ± 1.5 | 4.1 ± 1.9 | 2.9 ± 1.2 |
| Hypertension (%) | 30 | 25 | 35 |
| Diabetes mellitus (%) | 20 | 15 | 25 |
| Total cholesterol (mg/dL) | 236 ± 32 | 231 ± 38 | 239 ± 41 |
| LDL cholesterol (mg/dL) | 139 ± 30 | 136 ± 38 | 144 ± 28 |
| Triglycerides (mg/dL) | 148 (78, 201) | 140 (76, 192) | 151 (81, 220) |
| Systolic BP (mmHg) | 120 ± 20 | 118 ± 22 | 124 ± 18 |
| Diastolic BP (mmHg) | 76 ± 12 | 74 ± 10 | 78 ± 14 |
| Heart rate (beat/min) | 64 ± 10 | 60 ± 10 | 68 ± 12 |
| Medication (%) | | | |
| ACEI/ARB | 98 (58/40) | 95 (54/41) | 100 (62/38) |
| Diuretics | 88 | 90 | 86 |
| Digoxin | 68 | 72 | 64 |
| β-blocker | 78 | 82 | 74 |

Values are mean ± SD or median (25th, 75th percentile). P values for all data between the 2 groups were not significant. CHF, congestive heart failure ; BP, blood pressure ; ACEI, angiotensin-converting enzyme inhibitors ; ARB, angiotensin II receptor blockers.

heart failure complications (CAD(+) group), and 19 patients in the control group (CAD(−) group) with complications of non-ischemic heart failure (valvular disorder, arrhythmia, etc.). Patient backgrounds such as age, sex, and co-morbidities, were considered.

Lipid parameters including blood TC, LDL-C, HDL-C, and TG, were monitored before and 6, and 12 months after pitavastatin administration. Heart failure related parameters such as plasma concentration of brain natriuretic peptide (BNP) and left ventricular ejection fraction (LVEF) were monitored before and 12 months after the administration. Plasma concentration of BNP was assayed using a chemiluminescent enzyme immunoassay (SRL, Tokyo, Japan). LVEF was estimated by M-mode and 2-dimensional echocardiography (Xario, Toshiba, Japan).

Participants' written informed consent and local institutional review board approvals were obtained before the study.

**Statistical analysis** : One-sample t-test was utilized to assess effectiveness before and after pitavastatin administration. In either method, values below 5% on 12 months were considered statistically significant, and readings were recorded as mean ± SD.

## Results

Patient backgrounds for the 38 patients enrolled are shown in **Table 1**. There were no significant differences in age, sex, lipid profiles, hemodynamic parameters, LVEF (**Table 2**), or medications between the CAD (+) and CAD(−) groups.

After treatment, the serum levels of TC and LDL-C concentration significantly decreased in the both groups. The serum levels of HDL-C concentration significantly increased in the both groups after treatment. There were no significant differences in the lipid profile comparing the two groups (**Table 2**). The plasma BNP levels decreased in the both groups, and the BNP level in the CAD(+) group showed a tendency for decrease compared with the CAD(−) group after 12 months (−82 [−410, 145] vs. −43 [−306, 180]) (**Figure 1A**).

Cardiac function improved in both groups following treatment with pitavastatin. The LVDd and LVDs significantly decreased, and the LVEF significantly in-

Table 2 Serial changes of several variables in patients with CHF

| | CAD(−) (n=19) | | | CAD(+) (n=19) | | |
|---|---|---|---|---|---|---|
| | Baseline | 6 m | 12 m | Baseline | 6 m | 12 m |
| NYHA | 2.2±0.8 | 2.0±0.6 | 2.0±0.6 | 2.0±0.6 | 1.8±0.6 | 1.8±0.6 |
| SBP(mmHg) | 118±22 | 114±20 | 112±18 | 124±18 | 118±16 | 116±18 |
| DBP(mmHg) | 74±10 | 72±12 | 74±12 | 78±14 | 76±12 | 74±10 |
| HR(beat/min) | 60±10 | 64± 8 | 62±10 | 68±12 | 72±10 | 74± 8 |
| TC(mg/dL) | 231±38 | 178±25* | 182±14* | 239±41 | 182±41* | 169±32† |
| LDL-C(mg/dL) | 136±38 | 87±12* | 88± 9 * | 144±28 | 94±17* | 83±12† |
| TG(mg/dL) | 140(76, 192) | 136(75, 160) | 135(76, 163) | 151(81, 220) | 137(78, 199) | 148(75, 186) |
| BNP(pg/mL) | 112(60, 244) | 80(30, 174) * | 69(36, 145) * | 122(90, 221) | 98(40, 221) * | 40(24, 180) * |
| LVDd(mm) | 60.2(58.0, 70.4) | 58.0(56.9, 68.2) * | 57.4(55.6, 66.8) * | 59.1(55.4, 69.1) | 58.0(53.4, 66.2) * | 56.2(53.4, 63.0) * |
| LVDs(mm) | 55.5(48.2, 60.4) | 53.3(46.9, 58.4) * | 51.4(45.5, 56.8) * | 53.6(47.4, 59.9) | 49.8(45.8, 56.9) * | 47.8(44.1, 55.2) * |
| LVEF(%) | 40.6±7.8 | 41.3±7.2 | 43.0±6.7* | 40.5±8.0 | 48.8±9.6* | 45.2±11.7* |

Values are mean ± SD or median (25th, 75th percentile). SBP, systolic blood pressure ; DBP, diastolic blood pressure ; HR, heart rate ; TC, total cholesterol ; LDL-C, LDL cholesterol ; TG, triglycerides.
* : $p<0.05$ vs baseline, † : $p<0.01$ vs baseline.

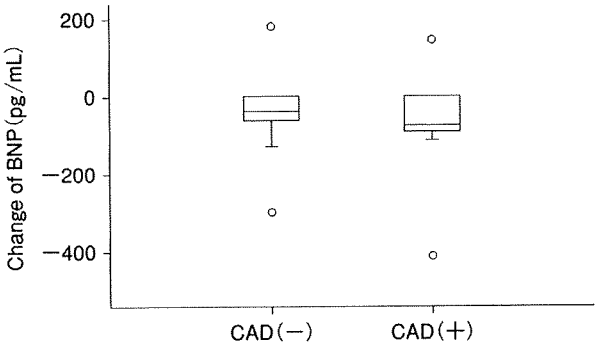


Figure 1A Comparison of the changes in plasma level of BNP between CAD(−) group and CAD (+) group 12 months after treatment

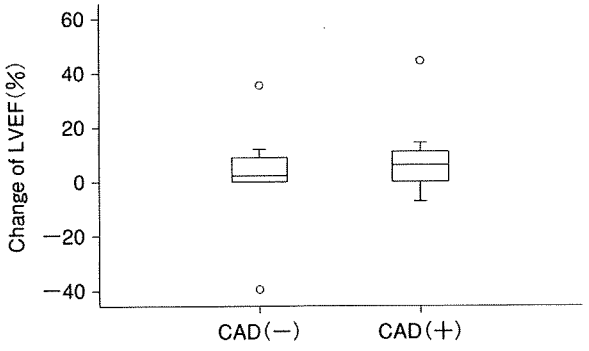


Figure 1B Comparison of the changes in LVEF between CAD(−) group and CAD(+) group 12 months after treatment

creased in the both groups after treatment (Figure 1 B). The CAD(+) group showed a tendency for the increase in LVEF greatly compared with the CAD(−) group (7.0 [2.0, 44.9] vs. (2.8 [−38.9, 35.5]) after 12 months (Figure 1B). No major adverse events were observed.

## Discussion

It has been reported that pitavastatin improved cardiac function in patients with heart failure[16]. In this study, we analyzed lipid profile and cardiac functional parameters between the ischemic heart failure complications (CAD(+) group) and the control group (CAD(−) group). Comparative analysis was conducted for each parameter before and after pitavastatin administration. In this study, both TC and LDL-C levels experienced statistically significant improvements and HDL-C levels for the CAD(+) group increased after 12 months. The TG levels before administration were variable, and no statistically significant changes were observed in either group.

Pitavastatin administration decreased the BNP level and increased LVEF in both groups, especially in the CAD(+) group. BNP is a useful peptide marker in everyday clinical practice to monitor heart failure, as well as for diagnosis of cardiac disease and heart failure. BNP belongs to the natrium peptide (NP) family. The NP system, derived from the NP family, and NP receptors possess strong natriuretic and vasodilating properties, as well as strong suppressive effects on renin-angiotensin system and sympathetic nervous

system. BNP is primarily synthesized in the ventricle, and is released into the vasculature in response to excessive stretching of myocytes[17].

The authors suggested the reason BNP levels decreased and LVEF increased in both groups was similar to the *in vivo* findings of pitavastatin administration in experimental dog models with heart failure[9]. In the dog model, pitavastatin improved left ventricular diastolic function and vascular endothelial function. A recent study reported that pitavastatin therapy in angiotensin Ⅱ (Ang Ⅱ)-induced left ventricular hypertrophy improved diastolic dysfunction and attenuated cardiac fibrosis, cardiomyocyte hypertrophy, coronary perivascular fibrosis, and medial thickening[18]. Ang Ⅱ-induced oxidative stress, cardiac transforming growth factor (TGF) $\beta$1 expression, and Smad 2/3 phosphorylation were all attenuated by pitavastatin. In this fashion, pitavastatin may improve LVEF through inhibition of the TGF-$\beta$-Smad 2/3 signaling pathway. Alternatively, rosuvastatin, a potent statin analog, is also reported to decrease hospitalization rate due to cardiac disease in elderly patients with heart failure, but to be ineffective in suppressing cardiovascular events[19]. Further prospective analysis is necessary.

Particularly, in the CAD (+) group, BNP level decreased whereas the LVEF level improved. BNP and p53 expression are reported to change dynamically under critical condition such as ACS[13,14,20], and perhaps under such conditions, agents such as pitavastatin, which suppresses p53, may provide higher treatment effects.

While only a hypothesis at present, as p53 is difficult to measure in actual clinical practice, pitavastatin holds the possibility of improving the prognosis of heart failure arising from ischemic cardiac disorders, as it improved BNP levels, which is a highly sensitive marker for sudden death after ischemic cardiac disorder, and which also reflects the prognosis of myocardial infarction.

In this study, pitavastatin administration for 12 months to patients with cardiac disorder who also suffered from a lipid metabolism abnormality was retrospectively analyzed. BNP level and LVEF transition differed from CAD(−) group and CAD(+) group, but further analysis is necessary with larger population. Currently, results are awaited from the PEARL study, lead by Komuro et al, which investigates the effect of pitavastatin on patients with chronic heart failure.

## References


1) Towbin JA, Bowles NE : The failing heart. Nature 2002 ; **415** : 227-233.
2) Sano M, Minamino T, Toko H, et al : p53-induced inhibition of Hif-1 causes cardiac dysfunction during pressure overload. Nature 2007 ; **446** : 444-448.
3) Fukuta H, Sane DC, Brucks S, et al : Statin therapy may be associated with lower mortality in patients with diastolic heart failure : a preliminary report. Circulation 2005 ; **112** : 357-363.
4) Kearney PM, Blackwell L, Collins R, et al ; Cholesterol Treatment Trialists' (CTT) Collaborators : Efficacy and safety of cholesterol lowering treatment : prospective meta-analysis of data from 90,056 participants in 14 randomised trials of statins. Lancet 2005 ; **366** : 1267-1278.
5) Lipinski MJ, Abbate A, Fuster V, et al : Drug insight : statins for nonischemic heart failure—evidence and potential mechanisms. Nat Clin Pract Cardiovasc Med 2007 ; **4** : 196-205.
6) Merla R, Daher IN, Ye Y, et al : Pretreatment with statins may reduce cardiovascular morbidity and mortality after elective surgery and percutaneous coronary intervention : clinical evidence and possible underlying mechanisms. Am Heart J 2007 ; **154** : 391-402.
7) Tousoulis D, Charakida M, Stefanadi E, et al : Statins in heart failure. Beyond the lipid lowering effect. Int J Cardiol 2007 ; **115** : 144-150.
8) Kibayashi E, Urakaze M, Kobayashi C, et al : Inhibitory effect of pitavastatin (NK-104) on the C-reactive-protein-induced interleukin-8 production in human aortic endothelial cells. Clin Sci 2005 ; **108** : 515-521.
9) Morikawa S, Takabe W, Mataki C, et al : The effect of statins on mRNA levels of genes related to inflammation, coagulation, and vascular constriction in HUVEC. J Atheroscler Thromb 2002 ; **9** : 178-183.
10) Takayama T, Wada A, Tsutamoto T, et al : Contribution of vascular NAD(P)H oxidase to endothelial dysfunction in heart failure and the therapeutic effects of HMG-CoA reductase inhibitor. Circ J 2004 ; **68** : 1067-1075.
11) Sanada S, Asanuma H, Minamino T, et al : Optimal windows of statin use for immediate infarct limitation : 5′-nucleotidase as another downstream molecule of

phosphatidylinositol 3-kinase. Circulation 2004 ; **110** : 2143-2149.
12) Tounai H, Hayakawa N, Kato H, et al : Immunohistochemical study on distribution of NF-kappaB and p53 in gerbil hippocampus after transient cerebral ischemia : effect of pitavastatin. Metab Brain Dis 2007 ; **22** : 89-104.
13) Gheorghiade M, Bonou RO : Chronic heart failure in the United States : a manifestation of coronary artery disease. Circulation 1998 ; **97** : 282-289.
14) Rossi ML, Marziliano N, Merlini PA, et al : Different quantitative apoptotic traits in coronary atherosclerotic plaques from patients with stable angina pectoris and acute coronary syndromes. Circulation 2004 ; **110** : 1767-1773.
15) Buerke M, Pruefer D, Sankat D, et al : Effects of aprotinin on gene expression and protein synthesis after ischemia and reperfusion in rats. Circulation 2007 ; **116** : I121-I126.
16) Aoyagi T, Nakamura F, Tomaru T, et al : Beneficial effects of pitavastatin, a 3-hydroxy-3-methylglutaryl coenzyme A reductase inhibitor, on cardiac function in ischemic and nonischemic heart failure. Int Heart J 2008 ; **49** : 49-58.
17) Levin ER, Gardner DG, Samson WK : Natriuretic peptides. N Engl J Med 1998 ; **339** : 321-328.
18) Yagi S, Aihara K, Ikeda Y, et al : Pitavastatin, an HMG-CoA reductase inhibitor, exerts e-NOS-independent protective actions against angiotensin II-induced cardiovascular remodeling and renal insufficiency. Circ Res 2008 ; **102** : 68-76.
19) Kjekshus J, Apetrei E, Barrios V, et al : Rosuvastatin in older patients with systolic heart failure. N Engl J Med 2007 ; **357** : 2248-2261.
20) Kwan G, Isakson SR, Beede J, et al : Short-term serial sampling of natriuretic peptides in patients presenting with chest pain. J Am Coll Cardiol 2007 ; **49** : 1186-1192.

ELSEVIER

International Journal of Cardiology 140 (2010) e23–e26

International Journal of Cardiology

www.elsevier.com/locate/ijcard

Letter to the Editor

# Buerger's disease-like vasculitis associated with Kimura's disease

Hiroyuki Takaoka [a], Hiroyuki Takano [a,*], Keiichi Nakagawa [a], Yoshio Kobayashi [a], Kenzo Hiroshima [b], Issei Komuro [a]

[a] *Department of Cardiovascular Science and Medicine, Chiba University Graduate School of Medicine, Chiba, Japan*
[b] *Department of Diagnostic Pathology, Chiba University Graduate School of Medicine, Chiba, Japan*

Received 29 May 2008; accepted 16 November 2008
Available online 7 January 2009

**Abstract**

A 46-year-old man was first diagnosed as Buerger's disease according to his clinical and radiological features because he had no evidence of parasitic, allergic and connective tissue disease. Soft subcutaneous nodules suspected of lymphadenopathy on the bilateral inguinal regions were recognized after admission. Positron emission tomography scan showed the increased uptake of $^{18}$F-fluoro-2-deoxyglucose in the bilateral inguinal regions. We finally diagnosed him as Kimura's disease based on pathologic findings and laboratory data, and started steroid therapy. The uptake of $^{18}$F-fluoro-2-deoxyglucose disappeared and his leg pain was improved after the treatment. This is the first case report presenting a patient of Kimura's disease with Buerger's disease-like vasculitis who was demonstrated by positron emission tomography.


*Keywords:* Buerger's disease; Eosinophilia; Kimura's disease; Positron emission tomography; Prednisolone

## 1. Introduction

Buerger's disease (BD) is a nonatherosclerotic inflammatory disorder of unknown etiology that affects small and medium-sized vessels of the extremities. The diagnosis of BD requires the elimination of many other diseases because of the absence of specific diagnostic criteria. Kimura's disease (KD) is a rare chronic inflammatory disorder presenting subcutaneous masses predominantly in the head and neck region, and peripheral eosinophilia. Positron emission tomography (PET) scan is a powerful imaging technique in the diagnosis and follow-up of many diseases including cancer, infection and inflammation. We report a case of KD with BD-like vasculitis who was demonstrated by $^{18}$F-fluoro-2-deoxyglucose (FDG)-PET.

## 2. Case report

A 46-year-old man was admitted with a 1-month history of sharp rest pain in right calf. He had ischemic ulceration between the third and fourth toes of his right foot (Figs. 1A and 2A). He has smoked 10 cigarettes or less per day for 25 years. The digital subtraction angiogram of the extremities showed multiple occlusions of the distal arteries including right anterior tibial artery, right posterior tibial artery, right peroneal artery, left anterior tibial artery and left peroneal artery (Fig. 3). He was first diagnosed as BD according to his clinical and radiological features because he had no evidence of parasitic, allergic and connective tissue disease. Soft subcutaneous nodules suspected of lymphadenopathy on the bilateral inguinal regions were recognized after admission. No other lymph node was palpable. PET using FDG performed after overnight fasting and heparin sodium injection (2000 IU) revealed increased uptake of FDG in the bilateral inguinal regions (Fig. 4A). Since these lesions were considered as lymphoproliferative disorder, an excision biopsy of left inguinal nodule was performed. The pathology of the specimen revealed hyperplasia of lymphoid follicles

* Corresponding author. Department of Cardiovascular Science and Medicine, Chiba University Graduate School of Medicine, 1-8-1 Inohana, Chuo-ku, Chiba 260-8670, Japan. Tel.: +81 43 226 2097; fax: +81 43 226 2557.
*E-mail address:* htakano-cib@umin.ac.jp (H. Takano).

0167-5273/$ - see front matter © 2008 Elsevier Ireland Ltd. All rights reserved.
doi:10.1016/j.ijcard.2008.11.072

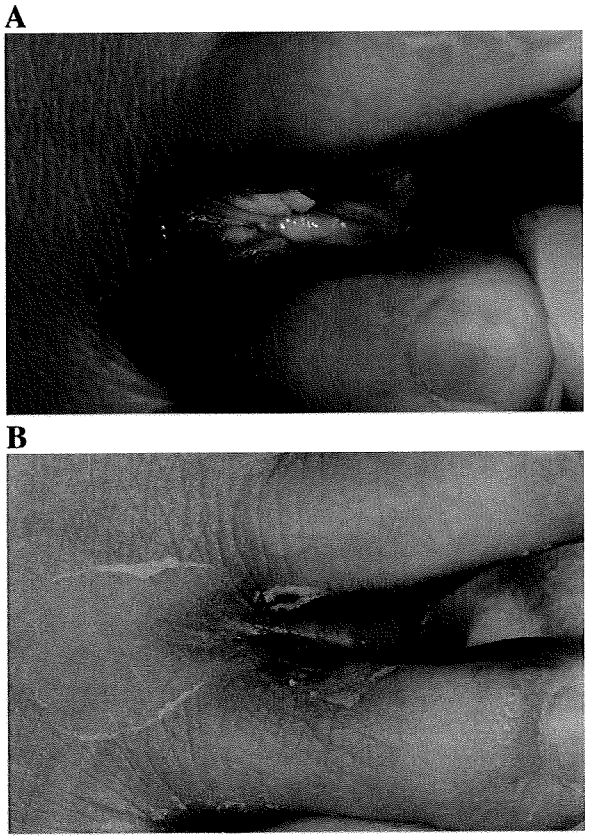


Fig. 1. Ischemic ulceration between the third and fourth toes of right foot (A) on admission and (B) after steroid therapy.

with germinal centers and massive infiltration of eosinophils without malignancy, which are typical findings of KD (Fig. 5A and B). Laboratory tests showed peripheral eosinophilia (WBC 20800, 56% eosinophils) and elevated serum immunoglobulin E level of 1921 U/mL. Screening for rheumatoid factor, anti-nuclear antibodies and ANCA were all negative. Protein C and protein S were within normal ranges. We finally diagnosed him as KD based on pathologic findings and laboratory data, and started the treatment with prednisolone 40 mg/day. After the treatment, eosinophilia, the ulcer and rest pain of right foot improved quickly (Figs. 1B and 2B). The FDG uptake in the bilateral inguinal regions disappeared after 4 weeks by the treatment with prednisolone (Fig. 4B).

## 3. Discussion

BD is a nonatherosclerotic inflammatory disorder of unknown etiology that affects small and medium-sized vessels of the extremities and has a strong association with smoking [1]. Typically, affected persons are young men and the symptoms appear before the age of 40 years old. Cessation of cigarette smoking is the only known effective therapy. The diagnosis of BD requires ruling out other diseases because of the absence of specific diagnostic criteria. KD is a rare chronic inflammatory disorder presenting subcutaneous masses predominantly in the head and neck region, peripheral eosinophilia and elevated serum immunoglobulin E level [2]. Histologically, lymphoid follicles formed from lymphocytes,

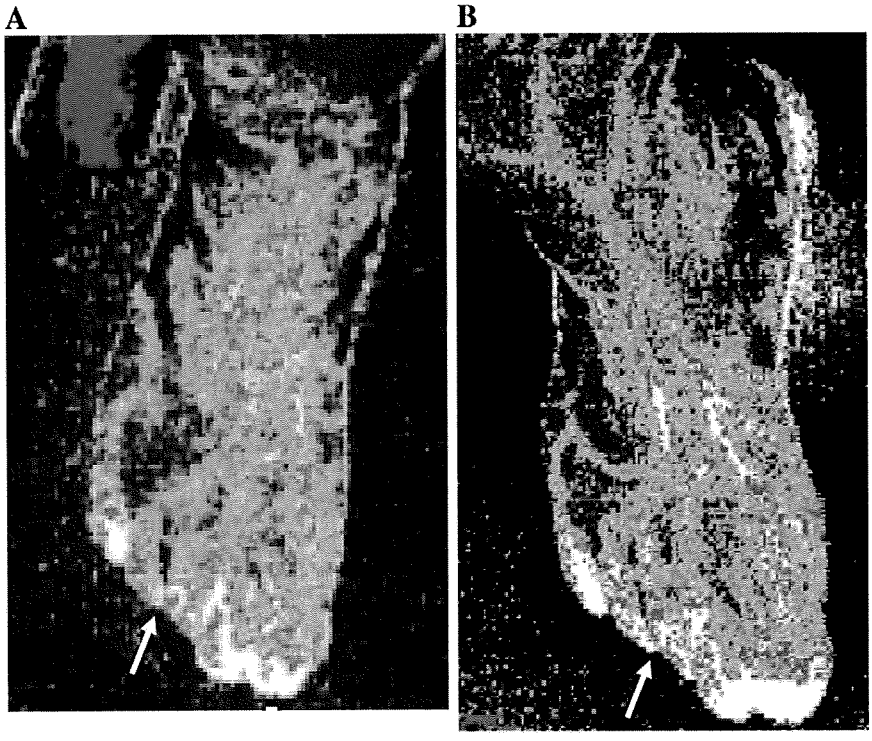


Fig. 2. Laser Doppler imaging of right foot (A) on admission and (B) after steroid therapy. Color-coded images represent blood flow distribution. The highest perfusion is displayed as white. The steroid therapy improved the peripheral blood supply (arrows).

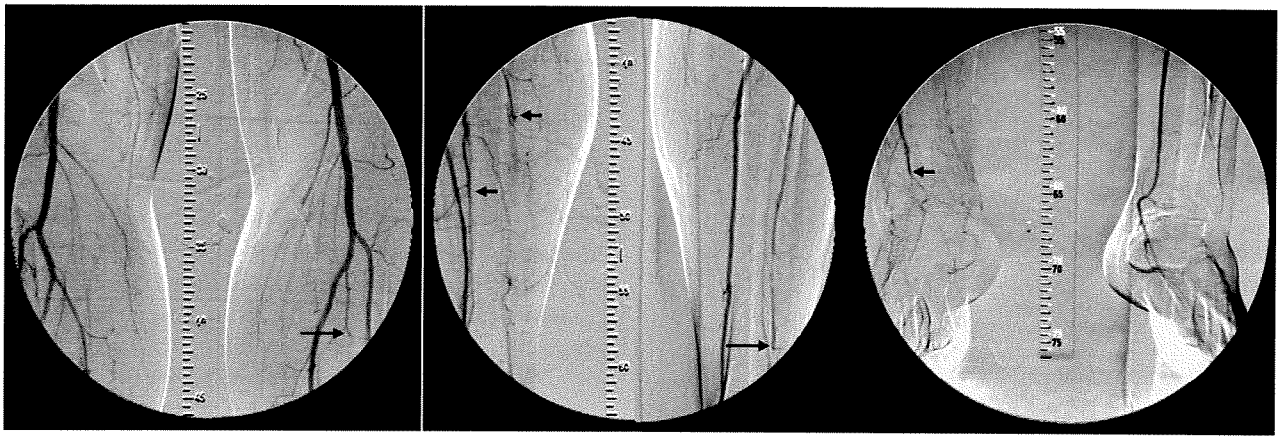

Fig. 3. Multiple occlusions of the crural arteries including right anterior tibial artery, right posterior tibial artery, right peroneal artery (arrowheads), left anterior tibial artery and left peroneal artery (arrows).

plasma cells and abundant eosinophils are characteristic. KD occurs endemically in Asian males. Renal abnormalities are associated with KD [3], but there is only one case on KD patient with BD [4]. PET scan is a powerful imaging technique in the diagnosis and follow-up of many diseases including cancer, infection and inflammation. Recently, the generalized lymphadenopathy was demonstrated in a patient with KD by FDG-PET [5]. In the present case, FDG-PET showed the increased uptake of FDG in the bilateral inguinal regions, which disappeared after steroid therapy. Concomitantly, the pain and ulceration of his right leg were improved. To our knowledge, there is no report presenting a patient of KD with BD-like vasculitis who was demonstrated by FDG-PET. Although the pathogenesis of BD is still unknown, steroid therapy is effective to stabilize inflammation in the patients with BD-like vasculitis. Therefore, it is important to

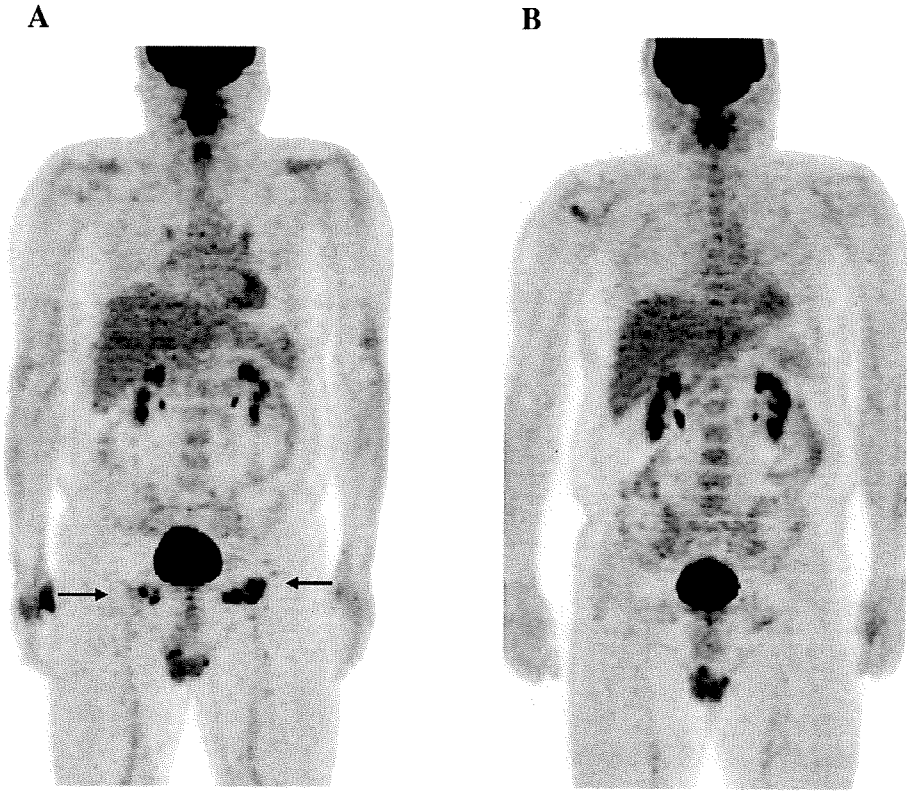


Fig. 4. FDG uptake (A) on admission and (B) after steroid therapy. The FDG uptake in the bilateral inguinal regions (arrows) disappeared 4 weeks after the steroid therapy.

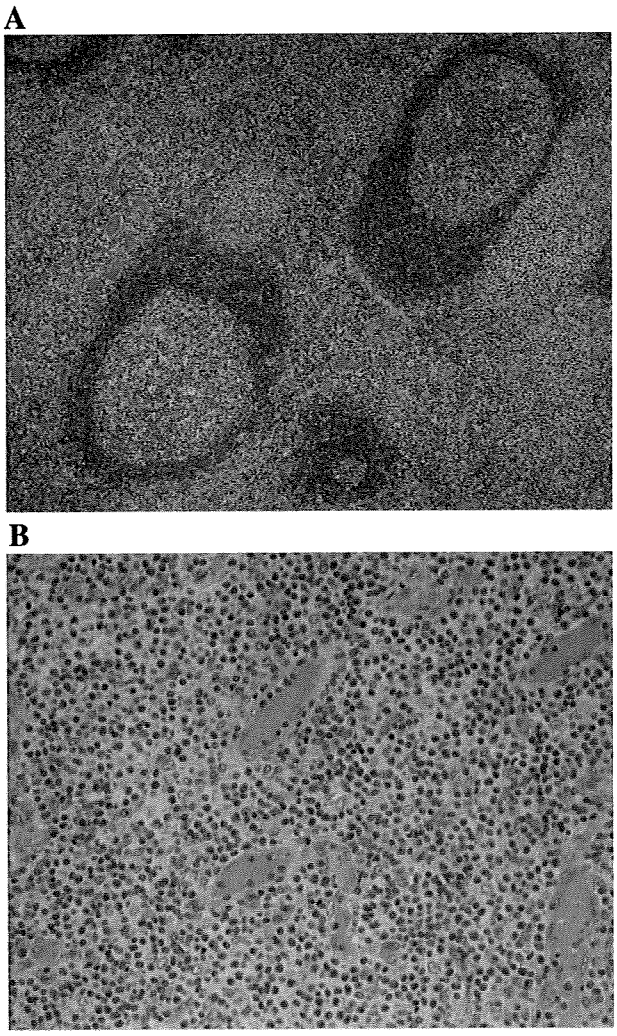


Fig. 5. Photomicrograph of the left inguinal nodule showed hyperplasia of lymphoid follicles with germinal centers and massive infiltration of eosinophils (hematoxylin and eosin staining). A, lower magnification, ×40. B, higher magnification, ×200.

examine the patients with vasculitis by FDG-PET whether they have lymphadenopathy or tumor-like lesion.

## Acknowledgement

The authors of this manuscript have certified that they comply with the Principles of Ethical Publishing in the International Journal of Cardiology [6].

## References

[1] Puéchal X, Fiessinger JN. Thromboangiitis obliterans or Buerger's disease: challenges for the rheumatologist. Rheumatology 2007;46: 192–9.
[2] Abuel-Haija M, Hurford MT. Kimura disease. Arch Pathol Lab Med 2007;131:650–1.
[3] Nakahara C, Wada T, Kusakari J, et al. Steroid-sensitive nephrotic syndrome associated with Kimura disease. Pediatr Nephrol 2000;14:482–5.
[4] Nagashima T, Kamimura T, Nara H, Iwamoto M, Okazaki H, Minota S. Kimura's disease presenting as steroid-responsive thromboangiitis obliterans. Circulation 2006;114:e10–1.
[5] Wang TF, Liu SH, Kao CH, Chu SC, Kao RH, Li CC. Kimura's disease with generalized lymphadenopathy demonstrated by positron emission tomography scan. Intern Med 2006;45:775-758.
[6] Coats AJ. Ethical authorship and publishing. Int J Cardiol 2009;131:149–50.

# Right-Sided Heart Wall Thickening and Delayed Enhancement Caused by Chronic Active Myocarditis Complicated by Sustained Monomorphic Ventricular Tachycardia

Yoshiyuki Hama, MD; Nobusada Funabashi, MD; Marehiko Ueda, MD; Tomonori Kanaeda, MD; Masae Uehara, MD; Koki Nakamura, MD; Taichi Murayama, MD; Yoko Mikami, MD; Hiroyuki Takaoka, MD; Miyuki Kawakubo, MD; Kwangho Lee, MD; Hiroyuki Takano, MD; Issei Komuro, MD

An asymptomatic healthy 65-year-old man was referred to a hospital for inverted T waves in the precordial leads (Figure 1) with paroxysmal advanced atrioventricular block in the ECG. Chest x-ray showed mild cardiac enlargement (Figure 2), and an echocardiogram showed right ventricular (RV) wall thickening (arrow in Figure 3). Five months later, the patient was referred to another hospital complaining of chest discomfort. Coronary angiogram was normal, but sustained monomorphic ventricular tachycardia (VT) occurred. Suffering from incessant VT, the patient was transferred to our hospital. The ECG and echocardiogram were almost the same as in previous studies. Enhanced multislice computed tomography revealed isolated right atrial, RV, and partial left ventricular (LV) wall thickening with extensive delayed enhancement (Figure 4) but no other organic diseases, which was confirmed by cardiac magnetic resonance (Figure 5).

In an electrophysiological study, 2 sustained monomorphic VTs (Figure 6) were induced, located in the RV midseptum by endocardial ventricular mapping. Radiofrequency ablation was performed at both sites; subsequently, neither VT could be induced. Because of the multislice computed tomography and cardiac magnetic resonance findings, endocardial biopsies were obtained from the RV (Figure 7) that showed interstitial edema, fibrosis, and myocyte destruction with a dense infiltrate of lymphocytes, suggesting chronic active myocarditis, which was consistent with his clinical course. Presumably, the thickening of the right atrial and RV free walls is related to lymphocytic infiltration and edema in the multislice computed tomography and cardiac magnetic resonance. A cardioverter-defibrillator was implanted, and the patient was given 40 mg/d prednisolone. He had no recurrent VTs after discharge.

## Disclosures

None.

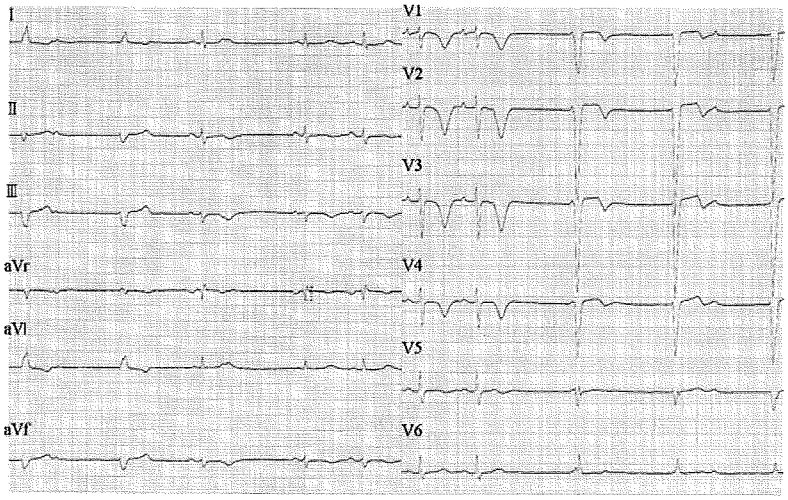


**Figure 1.** ECG acquired when the subject was referred to hospital showed inverted T waves in the precordial leads.

From the Department of Cardiovascular Science and Medicine, Chiba University Graduate School of Medicine, Chiba, Japan.
Correspondence to Issei Komuro, MD, PhD, Department of Cardiovascular Science and Medicine, Chiba University Graduate School of Medicine, Inohana 1–8–1, Chuo-ku, Chiba City, Chiba 260–8670, Japan. E-mail komurotky2000@yahoo.co.jp
(*Circulation.* **2009;119:e200-e203.**)


*Circulation* **is available at http://circ.ahajournals.org**

**DOI: 10.1161/CIRCULATIONAHA.108.788380**

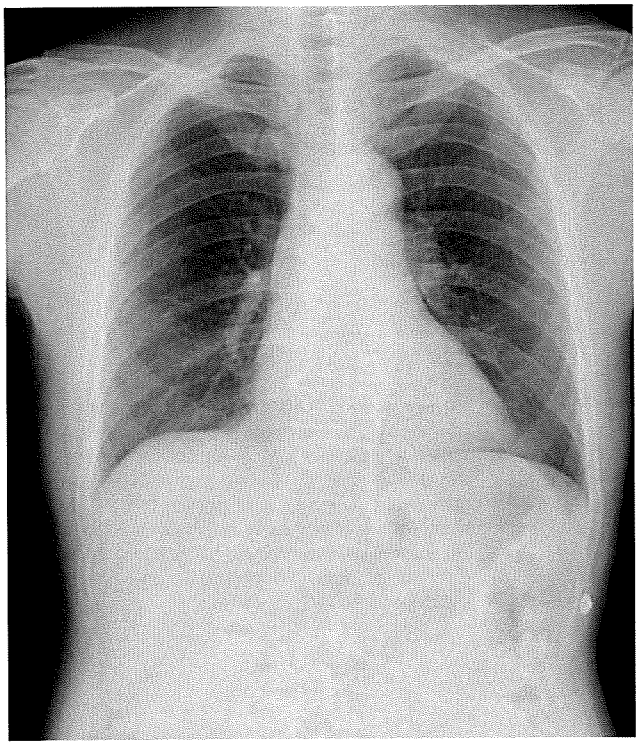

**Figure 2.** Chest x-ray showed mild cardiac enlargement.

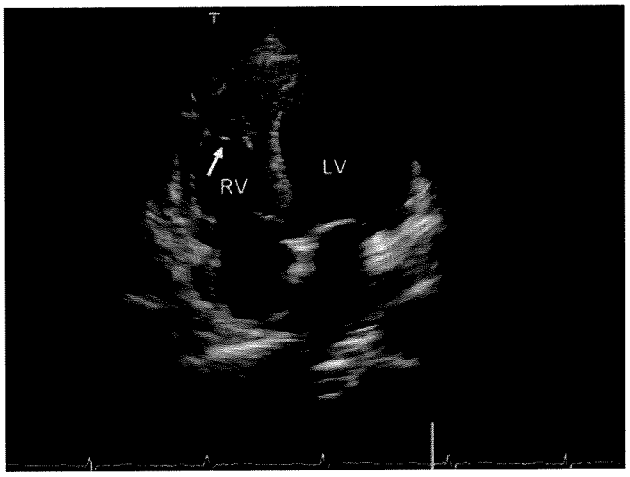


**Figure 3.** Transthoracic echocardiogram showed pericardial effusion and RV wall thickening (arrow) with no LV hypertrophy and normal systolic function of both ventricles.

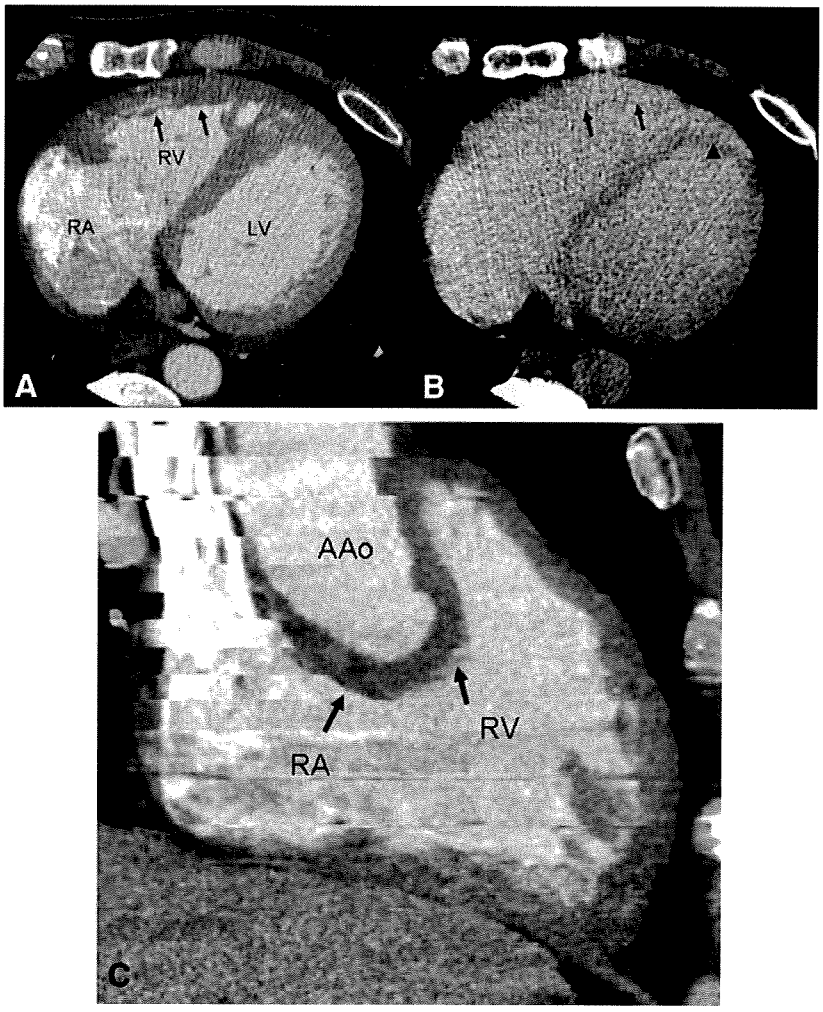


**Figure 4.** Axial source (A and B) and multiplanar reconstruction images (C) of enhanced multislice computed tomography revealed thickening of the right atrial (RA) and RV free walls (arrows in A and C) and part of the LV wall, which were abnormally enhanced in the later phase, as well as part of LV (arrows in B), suggesting lymphocytic infiltration and edema. AAo indicates ascending aorta.

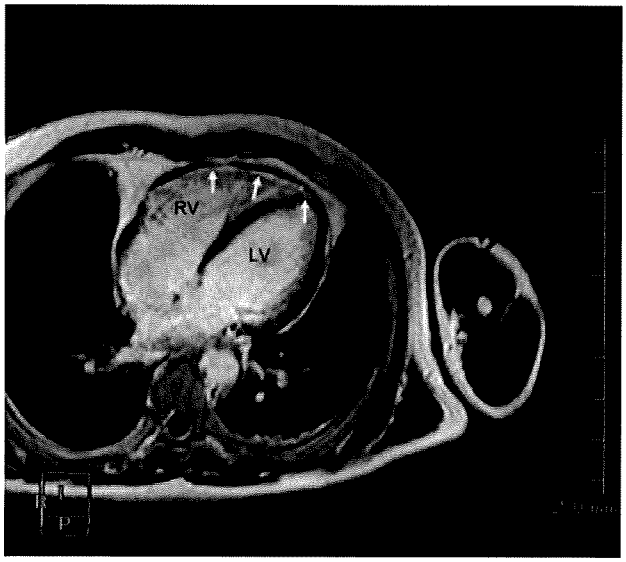


**Figure 5.** Cardiac magnetic resonance image revealed delayed enhancement (arrows) in the RV and part of the LV that was also observed in multislice computed tomography.

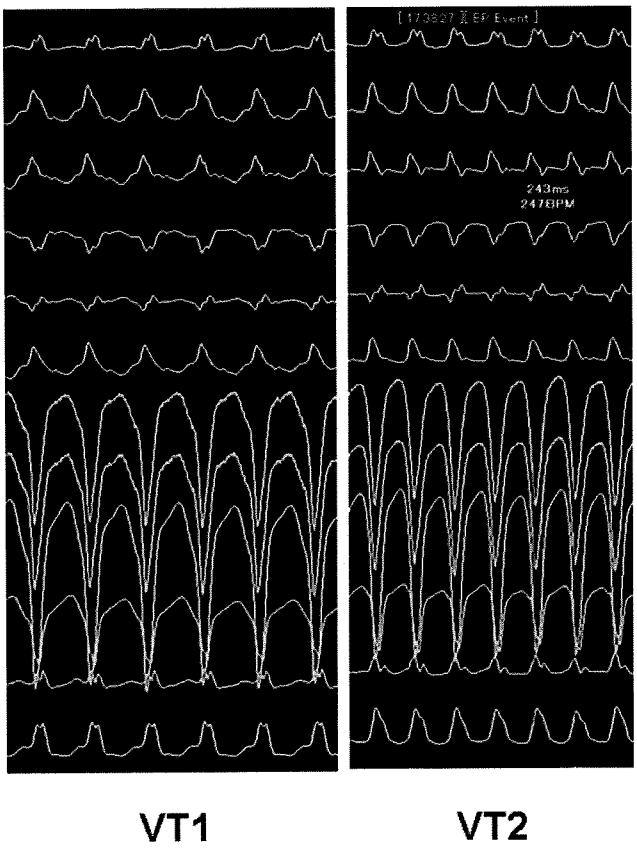


**Figure 6.** In an electrophysiological study, 2 clinical sustained monomorphic VTs were induced.

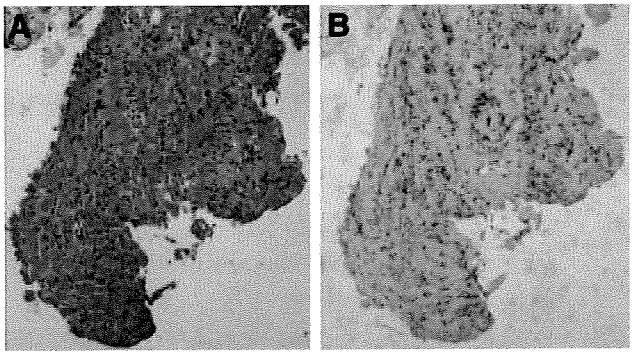


**Figure 7.** Histological results of endomyocardial biopsies. A, Hematoxylin and eosin staining demonstrated active myocarditis with focal lymphocytic infiltration with adjacent myocytolysis (×100). B, Immunohistological staining of T cells with focal infiltration pattern (×100).

*Circ J* 2009; **73:** 1762–1764

# Silent Very Late Thrombotic Occlusion of Sirolimus-Eluting Stent Confirmed by Directional Coronary Atherectomy

Takashi Nakayama, MD; Yoshio Kobayashi, MD; Hiroyuki Takano, MD; Nakabumi Kuroda, MD; Kenzo Hiroshima, MD*; Issei Komuro, MD

Stent thrombosis is defined as thrombotic occlusion of a stent resulting in acute coronary syndrome (ACS). However, all thrombotic occlusions of stents might not result in ACS. The present case report describes silent, very late thrombotic occlusion of a drug-eluting stent that was confirmed from specimens removed by directional coronary atherectomy. (*Circ J* 2009; **73:** 1762–1764)

**Key Words:** Angioplasty; Coronary artery disease; Restenosis; Stent; Stent thrombosis

Late stent thrombosis after drug-eluting stent (DES) placement has emerged as a major concern.[1–4] Stent thrombosis is defined as thrombotic occlusion of a stent resulting in acute coronary syndrome (ACS),[5–7] but all thrombotic occlusions of stents might not result in ACS. The present case report describes silent, very late thrombotic occlusion of DES that was confirmed from specimens removed by directional coronary atherectomy (DCA).[8,9]

## Case Report

A 61-year-old man with a history of hypertension was admitted because of exertional angina. Coronary angiography revealed 90% stenosis in the proximal left anterior descending coronary artery (LAD) and collaterals from the right coronary artery (**Figure 1A**), so the patient was referred for coronary angioplasty. An 18-mm sirolimus-eluting stent (SES, Cypher™, Cordis, Miami, FL, USA), premounted on a 3.5-mm balloon catheter, was deployed at 16 atm. The final angiogram (**Figure 1B**) and intravascular ultrasound (IVUS) (**Figure 2A**) showed a good result. He received ticlopidine (100 mg twice daily) plus aspirin (100 mg/day) for 3 months and thereafter was on aspirin monotherapy. Seven months later follow-up angiography demonstrated no in-stent restenosis (**Figure 1C**). Follow-up IVUS that was performed as part of clinical research demonstrated minimum intimal hyperplasia without incomplete apposition (**Figure 2B**).

Because of exertional angina persisting for several months, he was referred for coronary angiography 23 months after SES implantation. There were no electrocardiographic abnormalities to indicate ACS (**Figure 3**) or elevated levels of biomarkers for myocardial necrosis. Coronary angiography demonstrated total occlusion of the SES (**Figure 1D**) and complete filling of the LAD distal to the SES from the right coronary artery (**Figure 1E**). The patient was referred for coronary angioplasty. A 0.014-inch Conquest Pro guidewire (Asahi Intecc, Seto, Japan) supported with a tornus catheter (Asahi Intecc) was crossed through the total occlusion. Predilatation using a 2.0-mm Lacrosse balloon catheter (Goodman, Nagoya, Japan) inflated at 6 atm was performed. The guidewire was then changed to a flexi-wire (Guidant, Santa Clara, CA, USA). IVUS was performed and demonstrated a heterogeneous mass in the stent (**Figure 2C**). With the informed consent of the patient, DCA using a Flexicut directional atherectomy device (Guidant) was performed with the intention of obtaining tissue in the stent to clarify the mechanism of delayed total occlusion (**Figure 1F**)[8,9]; informed consent for a case report was obtained later. A total of 7 cuts were performed, inflating the balloon up to 50 psi. A 28-mm SES premounted on a 3.0-mm balloon catheter was then deployed at 18 atm. The final angiogram showed a good result (**Figure 1G**). Pathological examination of the DCA specimens demonstrated organized thrombus rather than neointima (**Figure 4**).

## Discussion

DES has dramatically reduced the incidence of in-stent restenosis,[6,7] but a new problem of late stent thrombosis has appeared.[1–4] Previous clinical studies used relatively restrictive and non-uniform definitions of stent thrombosis[6,7] These definitions uniformly regarded evidence of any myocardial infarction with angiographic confirmation of in-stent thrombus or unexplained death within 30 days after the procedure as stent thrombosis, but varied when myocardial infarction was present without angiographic confirmation of target-vessel involvement. Thus, standardized definitions of stent thrombosis were required and were recently proposed by the newly formed Academic Research Consortium (ARC).[5] Their definition of definite stent thrombosis requires the presence of ACS with angiographic or autopsy evidence of thrombus or occlusion. Probable

(Received March 25, 2008; revised manuscript received September 11, 2008; accepted September 16, 2008; released online January 14, 2009)
Department of Cardiovascular Science and Medicine, *Department of Diagnostic Pathology, Chiba University Graduate School of Medicine, Chiba, Japan
Grant: none.
Mailing address: Yoshio Kobayashi, MD, Department of Cardiovascular Science and Medicine, Chiba University Graduate School of Medicine, 1-8-1 Inohana, Chuo-ku, Chiba 260-8670, Japan. E-mail: yoshio.kobayashi@wonder.ocn.ne.jp

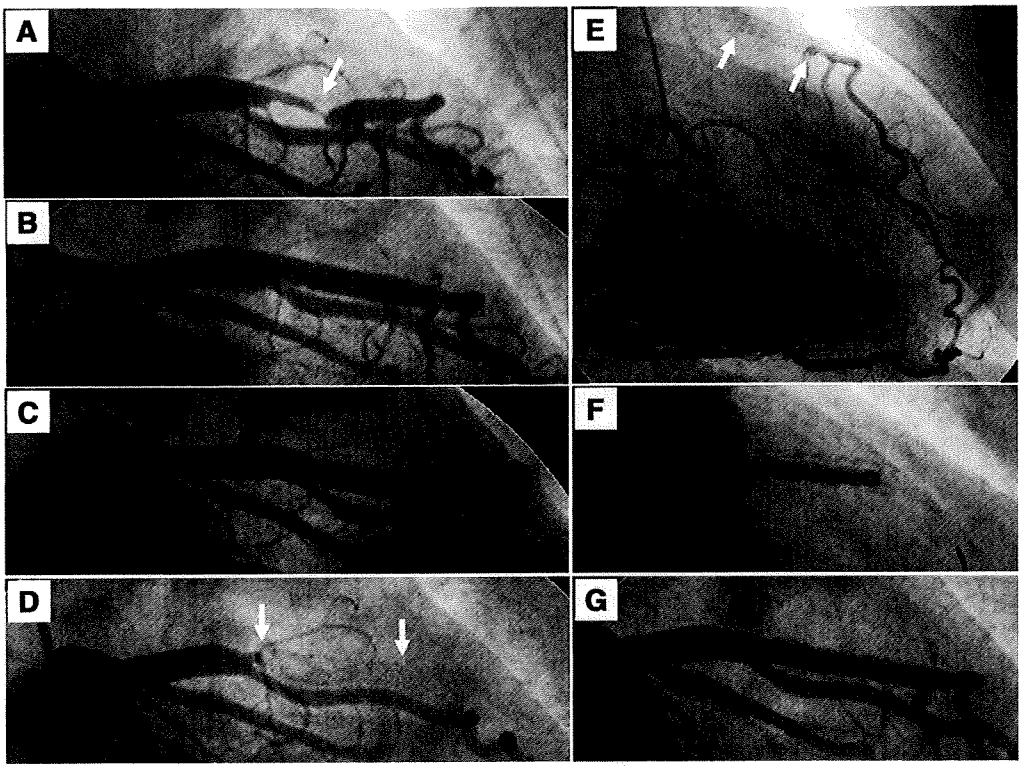


**Figure 1.** Coronary angiography showing 90% stenosis (arrow) of the proximal left anterior descending coronary artery (LAD) (**A**). After sirolimus-eluting stent (SES) implantation, angiography demonstrates a good result (**B**). Seven months later, follow-up angiography shows no in-stent restenosis (**C**). Coronary angiography demonstrates total occlusion of the SES (**D**) and complete filling of the LAD distal to the SES from the right coronary artery (**E**). Arrows (**D**,**E**) indicate the proximal and distal edges of the SES. Directional coronary atherectomy is performed (**F**) and the final angiogram shows a good result (**G**).

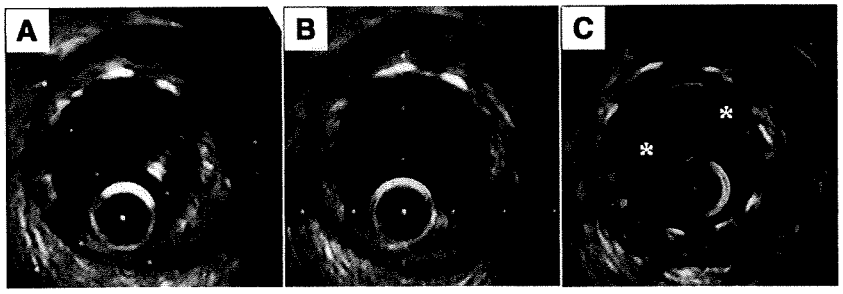


**Figure 2.** (**A**) Intravascular ultrasound (IVUS) after sirolimus-eluting stent implantation (stent cross-sectional area 7.6 $mm^2$). (**B**) Follow-up IVUS (stent cross-sectional area 7.7 $mm^2$). Note minimum intimal hyperplasia without incomplete apposition. (**C**) IVUS after predilatation for total occlusion (lumen cross-sectional area 2.6 $mm^2$ and stent cross-sectional area 7.7 $mm^2$). *Note heterogeneous mass in the stent.

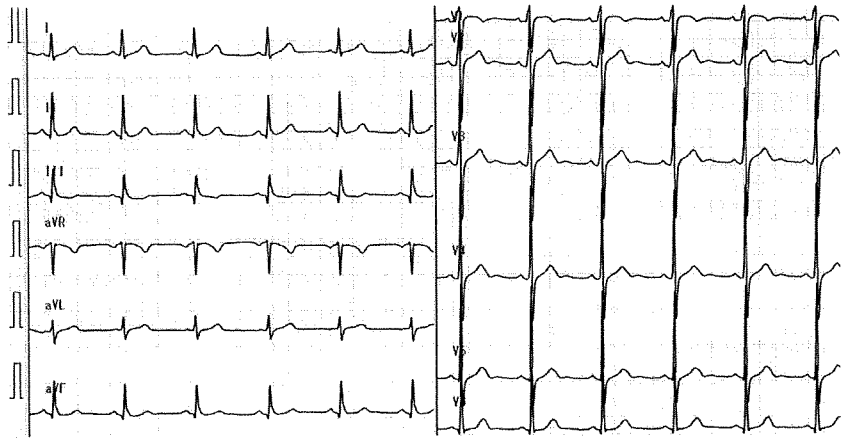


**Figure 3.** Electrocardiogram at 23 months after sirolimus-eluting stent implantation.

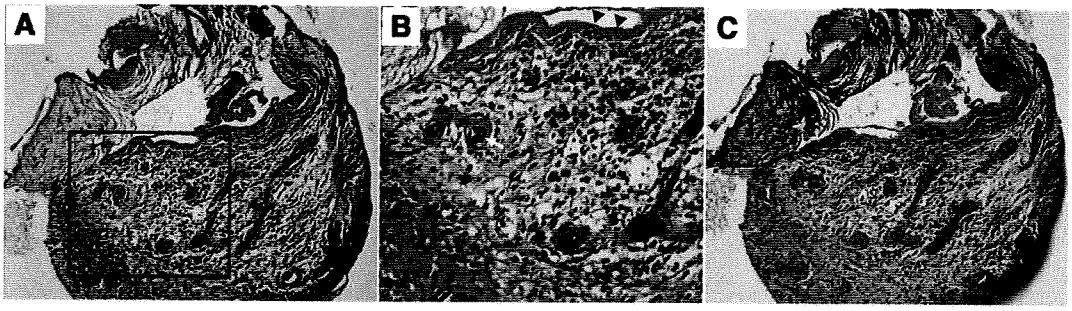


**Figure 4.** Hematoxylin and eosin (HE)-stained (**A**,**B**) and elastica van Gieson-stained (**C**) sections of a directional coronary atherectomy (DCA) specimen. (**B**) is a magnified view of the inset in (**A**). HE demonstrates fibrin (arrowheads), lymphocytes, fibroblast, hemosiderin-laden macrophages (black arrow) and neovascularization (white arrow). There are no smooth muscle cells and scant collagen fibers (red in **C**), which indicate that the DCA specimen is organized thrombus rather than neointima.

stent thrombosis includes unexplained death within 30 days after the procedure or acute myocardial infarction involving the target-vessel territory without angiographic confirmation. Possible stent thrombosis includes any unexplained death occurring at least 30 days after the procedure. Stent thrombosis was also classified as early (0–30 days), late (31–360 days) and very late (>360 days).

The reported incidence of late and very late stent thrombosis after DES implantation ranges between 0.2% and 0.7%.[1–3] In the present case, very late thrombotic occlusion of SES occurred in a patient without ACS, which might be considered as delayed in-stent restenosis (late catch-up phenomenon)[10] unless DCA and pathological examination were performed. According to the definitions of stent thrombosis by either previous clinical studies or the ARC,[5–7] the thrombotic occlusion of SES in the present case is not defined as stent thrombosis because the patient did not present with ACS. Thus, the incidence of thrombotic occlusion of DES may be higher than reported. There were well-developed collaterals in the present case, which might have prevented the patient from presenting with ACS. A previous study showed that, utilizing a sensor-tipped pressure guidewire, one-fifth of individuals without stenotic lesions had immediately recruitable collateral flow to the respective vascular area sufficient to prevent myocardial ischemia during a brief coronary occlusion.[11] In the present case, before SES implantation, collateral vessels from the right coronary artery supplied the distal LAD, so there may have been rapid recruitment of well-developed collaterals.[11,12] Gradual thrombus formation in SES, not resulting in sudden total occlusion, and recruitment of well-developed collaterals is another possibility for the patient not having presented with ACS. Silent thrombotic occlusion of a stent may occur in patients with no symptoms of myocardial ischemia (ie, some patients with diabetes mellitus or stent implantation in the infarct-related artery),[13] although the present case had exertional angina and did not have diabetes mellitus or a history of previous myocardial infarction.

## Conclusions

This case report shows very late thrombotic occlusion of DES in a patient without ACS, which was confirmed by specimens extracted by DCA. The incidence of very late thrombotic occlusion of DES might be higher than reported.

## References

1. Kitahara H, Kobayashi Y, Fujimoto Y, Nakamura Y, Nakayama T, Kuroda N, et al. Late stent thrombosis in patients receiving ticlopidine and aspirin after sirolimus-eluting stent implantation. *Circ J* 2008; **72:** 168–169.
2. Kuchulakanti PK, Chu WW, Torguson R, Ohlmann P, Rha SW, Clavijo LC, et al. Correlates and long-term outcomes of angiographically proven stent thrombosis with sirolimus- and paclitaxel-eluting stents. *Circulation* 2006; **113:** 1108–1113.
3. Iakovou I, Schmidt T, Bonizzoni E, Ge L, Sangiorgi GM, Stankovic G, et al. Incidence, predictors, and outcome of thrombosis after successful implantation of drug-eluting stents. *JAMA* 2005; **293:** 2126–2130.
4. Iwata Y, Kobayashi Y, Fukushima K, Kitahara H, Asano T, Ishio N, et al. Incidence of premature discontinuation of antiplatelet therapy after sirolimus-eluting stent implantation. *Circ J* 2008; **72:** 340–341.
5. Mauri L, Hsieh WH, Massaro JM, Ho KK, D'Agostino R, Cutlip DE. Stent thrombosis in randomized clinical trials of drug-eluting stents. *N Engl J Med* 2007; **356:** 1020–1029.
6. Moses JW, Leon MB, Popma JJ, Fitzgerald PJ, Holmes DR, O'Shaughnessy C, et al. Sirolimus-eluting stents versus standard stents in patients with stenosis in a native coronary artery. *N Engl J Med* 2003; **349:** 1315–1323.
7. Stone GW, Ellis SG, Cox DA, Hermiller J, O'Shaughnessy C, Mann JT, et al. A polymer-based, paclitaxel-eluting stent in patients with coronary artery disease. *N Engl J Med* 2004; **350:** 221–231.
8. Virmani R, Liistro F, Stankovic G, Di Mario C, Montorfano M, Farb A, et al. Mechanism of late in-stent restenosis after implantation of a paclitaxel derivate-eluting polymer stent system in humans. *Circulation* 2002; **106:** 2649–2651.
9. van Beusekom HM, Saia F, Zindler JD, Lemos PA, Swager-Ten Hoor SL, van Leeuwen MA, et al. Drug-eluting stents show delayed healing: Paclitaxel more pronounced than sirolimus. *Eur Heart J* 2007; **28:** 974–979.
10. Cosgrave J, Corbett SJ, Melzi G, Babic R, Biondi-Zoccai GG, Airoldi F, et al. Late restenosis following sirolimus-eluting stent implantation. *Am J Cardiol* 2007; **100:** 41–44.
11. Wustmann K, Zbinden S, Windecker S, Meier B, Seiler C. Is there functional collateral flow during vascular occlusion in angiographically normal coronary arteries? *Circulation* 2003; **107:** 2213–2220.
12. Perera D, Kanaganayagam GS, Saha M, Rashid R, Marber MS, Redwood SR. Coronary collaterals remain recruitable after percutaneous intervention. *Circulation* 2007; **115:** 2015–2021.
13. Xanthos T, Ekmektzoglou KA, Papadimitriou L. Reviewing myocardial silent ischemia: Specific patient subgroups. *Int J Cardiol* 2008; **124:** 139–148.

# Sonic hedgehog is a critical mediator of erythropoietin-induced cardiac protection in mice

Kazutaka Ueda,[1] Hiroyuki Takano,[1] Yuriko Niitsuma,[1,2] Hiroshi Hasegawa,[1] Raita Uchiyama,[1] Toru Oka,[1] Masaru Miyazaki,[2] Haruaki Nakaya,[3] and Issei Komuro[1]

[1]Department of Cardiovascular Science and Medicine, [2]Department of General Surgery, and [3]Department of Pharmacology, Chiba University Graduate School of Medicine, Chiba, Japan.

**Erythropoietin reportedly has beneficial effects on the heart after myocardial infarction, but the underlying mechanisms of these effects are unknown. We here demonstrate that sonic hedgehog is a critical mediator of erythropoietin-induced cardioprotection in mice. Treatment of mice with erythropoietin inhibited left ventricular remodeling and improved cardiac function after myocardial infarction, independent of erythropoiesis and the mobilization of bone marrow–derived cells. Erythropoietin prevented cardiomyocyte apoptosis and increased the number of capillaries and mature vessels in infarcted hearts by upregulating the expression of angiogenic cytokines such as VEGF and angiopoietin-1 in cardiomyocytes. Erythropoietin also increased the expression of sonic hedgehog in cardiomyocytes, and inhibition of sonic hedgehog signaling suppressed the erythropoietin-induced increase in angiogenic cytokine expression. Furthermore, the beneficial effects of erythropoietin on infarcted hearts were abolished by cardiomyocyte-specific deletion of sonic hedgehog. These results suggest that erythropoietin protects the heart after myocardial infarction by inducing angiogenesis through sonic hedgehog signaling.**

## Introduction

Recent medical advances have improved survival rates of patients with acute myocardial infarction (MI), whereas the number of patients showing heart failure after MI has increased in recent years (1). LV remodeling, which includes dilatation of the ventricle and increased interstitial fibrosis, is the critical process that underlies the progression to heart failure (1). Although pharmacological therapies are effective, heart failure is still one of the leading causes of death worldwide (2). It is thus important to elucidate a novel approach to prevent LV remodeling after MI.

Several hematopoietic cytokines including erythropoietin (EPO), G-CSF, and stem cell factor have been reported to prevent cardiac remodeling and dysfunction after MI in various animal models (3–5). EPO, a major regulator of erythroid progenitors, has attracted great attention because its administration induced significant improvements in the clinical status and LV function of patients with congestive heart failure (6, 7). Although several mechanisms of cardioprotective effects by EPO have been suggested, the precise mechanisms remain largely unknown (8–14). Treatment with EPO reverses the decreased oxygen-carrying capacity associated with anemia, which is often observed in patients with heart failure (8). EPO has also been reported to mobilize endothelial progenitor cells (EPCs) from bone marrow, leading to neovascularization in the heart (9). In addition, since EPO receptors (EPORs) are expressed in various types of cells including cardiomyocytes, EPO may have direct protective effects on cardiomyocytes (10–14).

In the present study, we investigated the mechanisms of how EPO induced cardioprotection after MI. We observed that EPO directly prevented apoptotic death of cardiomyocytes and enhanced the expression of angiogenic cytokines, which induced robust angiogenesis, leading to the improvement of contractile function after MI. EPO also increased expression levels of sonic hedgehog (Shh) in cardiomyocytes, and the inhibition of Shh signaling abolished the EPO-induced increases of angiogenic cytokine production in cardiomyocytes. In hearts of cardiac-specific inducible Shh knockout (Shh-MerCre) mice, EPO treatment failed to upregulate angiogenic cytokines, enhance angiogenesis, and inhibit LV remodeling. Our results suggest that Shh is a key mediator of EPO-evoked cardioprotection in infarcted hearts.

## Results

*EPO prevents cardiac remodeling after MI.* We subcutaneously administered EPO (10,000 U/kg/d) or saline immediately after coronary artery ligation until 4 days after MI. Fourteen days after MI, we histologically assessed the infarct size and examined cardiac function using echocardiography. Treatment with EPO significantly prevented enlargement of LV end-diastolic dimension (LVEDD) and reduction of fractional shortening (FS) and reduced the infarct size (fibrotic area/LV free wall) compared with saline treatment (Figure 1, A and B), suggesting that EPO prevents LV remodeling and dysfunction after MI.

The role of hematopoietic effects of EPO in cardioprotection (6, 7) was examined using transgene-rescued EPOR-null (RES) mice, which express EPORs only in the hematopoietic lineage (15). Although EPO treatment increased blood hemoglobin levels 7 days after MI in both WT and RES mice (Figure 2A), the cardioprotective effects of EPO were observed only in WT mice but not in the RES mice (Figure 1 and Figure 2B). EPO and saline did not show any significant differences in LVEDD, FS, or infarct size in the RES mice (Figure 2B), suggesting that erythropoiesis is not involved in the cardioprotective effects of EPO.

**Authorship note:** Kazutaka Ueda, Hiroyuki Takano, and Yuriko Niitsuma contributed equally to this work.

**Conflict of interest:** The authors have declared that no conflict of interest exists.

**Citation for this article:** *J Clin Invest* doi:10.1172/JCI39896.

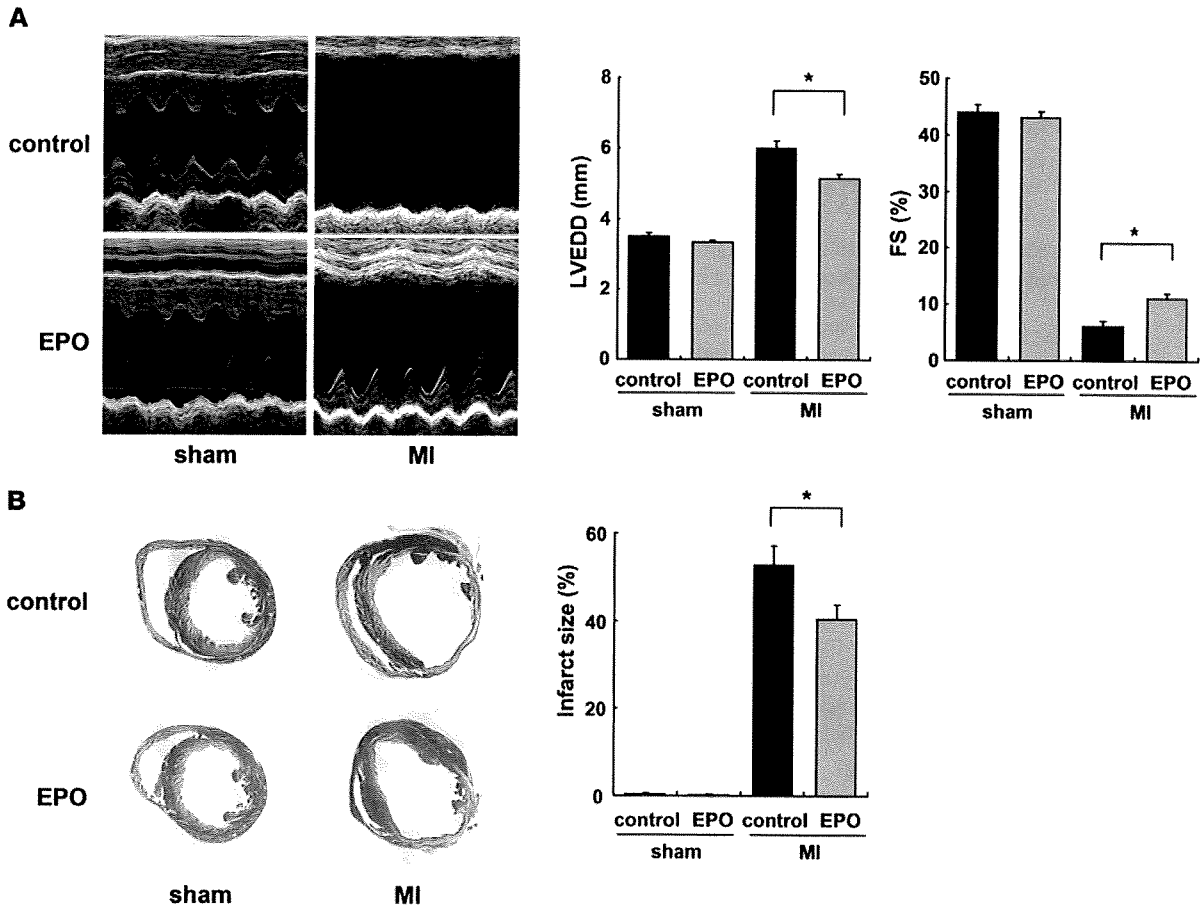


**Figure 1**
EPO prevents cardiac remodeling after MI. The effects of EPO treatment on LV function and infarct size were examined 14 days after operation. WT mice were subjected to MI or sham operation and treated with EPO or saline (control). (**A**) Echocardiographic analysis. ($n$ = 8–10). (**B**) Masson trichrome staining of hearts and infarct size ($n$ = 8–10). *$P$ < 0.01.

To investigate whether EPO affects responses of inflammation and wound healing that may have an impact on LV remodeling after MI (16, 17), we examined macrophage infiltration and myofibroblast accumulation in the ischemic area after MI by immunohistochemical staining. The number of Mac3-positive macrophages was markedly decreased by EPO treatment 14 days after MI (Supplemental Figure 1A; supplemental material available with this article; doi:10.1172/JCI39896DS1). The number of α-SMA–positive myofibroblasts was significantly increased in EPO-treated hearts compared with saline-treated hearts (Supplemental Figure 1B).

We next determined whether EPO induced the mobilization of EPCs from bone marrow into peripheral blood using flow cytometry (9). After MI, EPO significantly increased the number of circulating CD34/Flk-1–double-positive EPCs in WT mice but not in the RES mice (Figure 2C). We produced MI in WT mice in which the bone marrow was replaced with cells derived from GFP-expressing mice. The hearts were excised 7 and 14 days after MI and immunohistochemically stained for PECAM. There were no differences in the number of GFP-positive cells and GFP/PECAM–double-positive cells in the border areas of EPO- and saline-treated infarcted hearts (Figure 2D), indicating that EPO did not enhance the homing of bone marrow–derived cells or increase the number of bone marrow–derived endothelial cells in the damaged hearts, although EPO induced mobilization of EPCs from bone marrow into peripheral circulation. In addition, EPO did not improve cardiac function or increase the number of vessels in infarcted hearts even in RES mice transplanted with bone marrow of WT mice (Figure 2E). It is thus unlikely that the EPO-mobilized bone marrow–derived cells contribute to the cardioprotective effects of EPO.

*EPO inhibits cardiomyocyte apoptosis in infarcted hearts.* Apoptotic death of cardiomyocytes has been suggested to cause LV remodeling and dysfunction (18). To determine the role of antiapoptotic effects of EPO in cardioprotection, we performed TUNEL staining of hearts 24 hours after MI. The number of TUNEL-positive cardiomyocytes in the border area was significantly smaller in EPO-treated mice than in saline-treated mice, while EPO treatment had no effect on cardiomyocyte apoptosis in RES mice (Figure 3A). Western blot analysis showed that EPO treatment markedly reduced the level of cleaved caspase-3 in hearts at 24 hours after MI (Figure 3B). TUNEL staining revealed that pretreatment with EPO significantly attenuated $H_2O_2$-induced apoptotic death in cultured cardiomyocytes of neonatal rats (Figure 3C). At 24 hours after exposing cardiomyocytes to $H_2O_2$, expression levels of the antiapoptotic protein Bcl-2 were decreased, whereas levels of cleaved caspase-3 were increased, and these changes were inhibited markedly by EPO pretreatment (Figure 3D). Annexin V staining

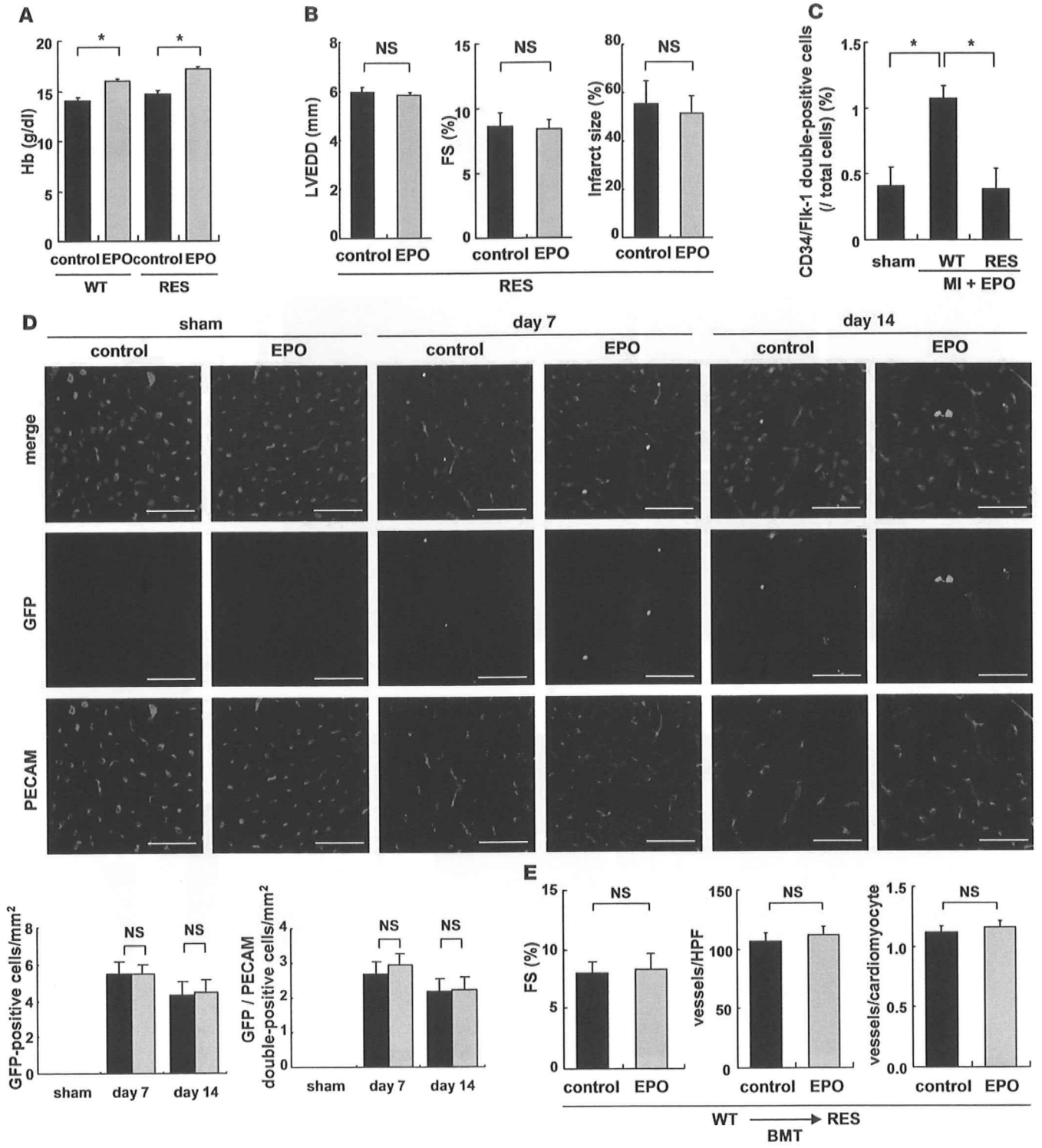


**Figure 2**

Erythroid hematogenesis is not required for the protective effects of EPO, and EPO does not accelerate the cardiac homing of bone marrow–derived cells after MI. WT and RES mice were subjected to MI and treated with EPO or saline (control). (**A**) Blood hemoglobin (Hb) levels 7 days after MI ($n = 4$). *$P < 0.01$. (**B**) Echocardiography and Masson trichrome staining were performed to analyze LV function and infarct size ($n = 10$). (**C**) Following MI and EPO treatment, the number of circulating CD34/Flk-1–double-positive EPCs increased in WT mice but not in RES mice. *$P < 0.05$ ($n = 4$). (**D**) Bone marrow cells from GFP-expressing mice were transplanted into WT mice. 7 and 14 days after MI, immunohistochemical staining for PECAM (red) was performed, and nuclei were counterstained with TO-PRO-3 (blue). GFP-positive cells (green) represent bone marrow–derived cells that moved into the heart and GFP/PECAM–double-positive cells denote bone marrow–derived endothelial cells. The numbers of GFP– and GFP/PECAM–double-positive cells in the border area (MI group) or LV free wall (sham group) were counted ($n = 5$–$8$). Scale bars: 50 μm. (**E**) WT bone marrow cells were transplanted (BMT) into RES mice, MI was induced, and the mice were treated with EPO or saline (control). FS, the number of vessels, and the ratio of vessels to cardiomyocytes in the border area are shown ($n = 8$).

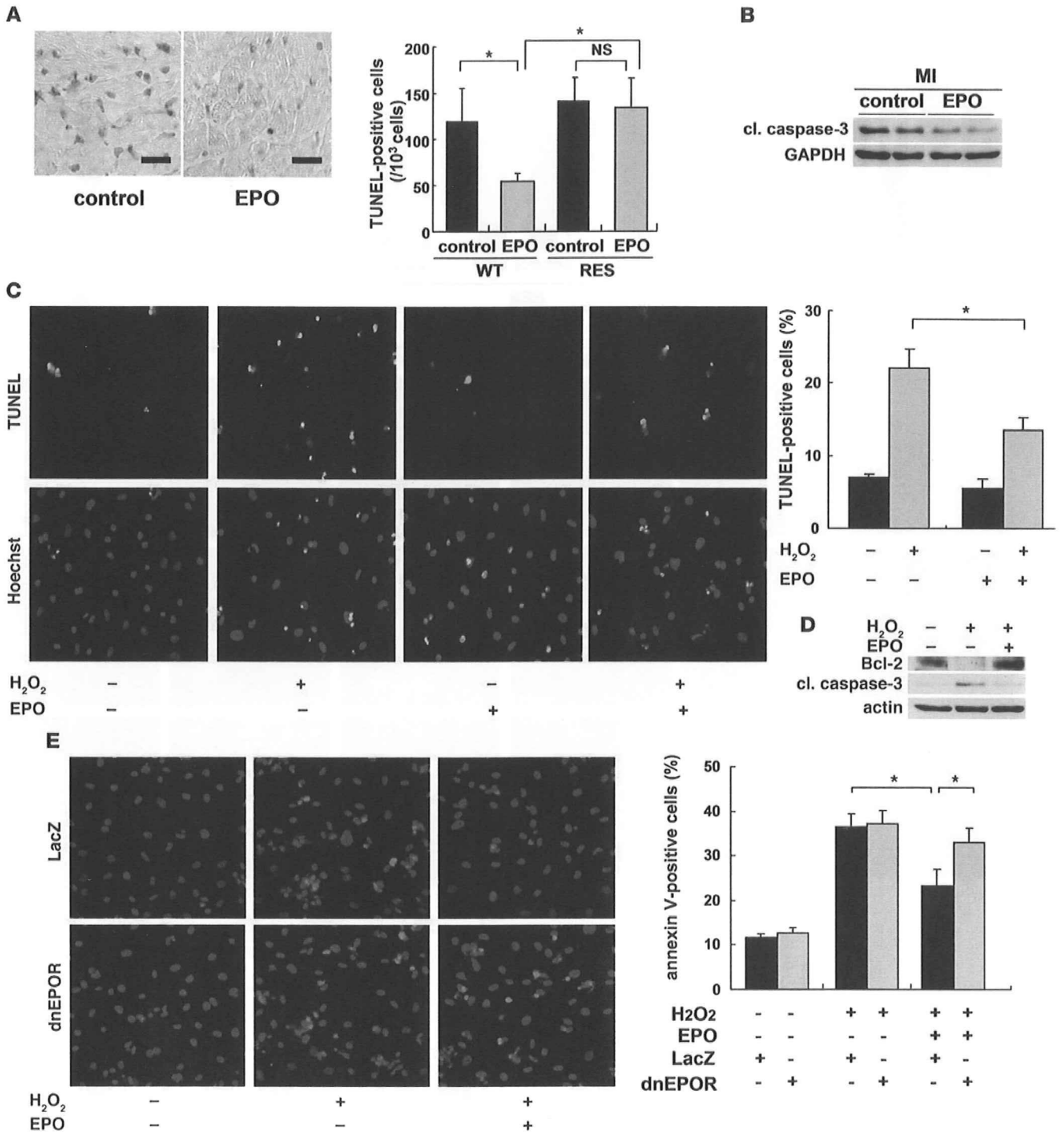


**Figure 3**

EPO inhibits cardiomyocyte apoptosis in infarcted hearts. (**A**) TUNEL staining (brown) of infarcted hearts from WT mice 24 hours after ligation. Scale bars: 100 μm. The number of TUNEL-positive cardiomyocytes in the border area was counted. *$P < 0.01$ ($n = 10$). (**B**) Representative Western blots of cleaved caspase-3 (cl. caspase-3) protein in the heart 24 hours after MI are shown ($n = 4$). (**C**) Detection of apoptotic cardiomyocytes using FITC-labeled TUNEL staining (green). Nuclei were counterstained with Hoechst 33258 (blue). The TUNEL-positive cardiomyocytes were counted ($n = 10$). *$P < 0.05$. (**D**) Samples were pretreated with EPO for 8 hours before $H_2O_2$ treatment, and the expression of Bcl-2 and cleaved caspase-3 24 hours after $H_2O_2$ treatment was analyzed by Western blotting. Representative results from 3 experiments are shown. (**E**) Detection of apoptotic cardiomyocytes using Cy-3–labeled annexin V staining (red). Nuclei were counterstained with Hoechst 33258 (blue). Cardiomyocytes were infected with adenoviral vectors encoding dominant negative form of EPOR or LacZ at 10 MOI. The number of annexin V–positive cardiomyocytes was counted ($n = 10$). *$P < 0.05$.

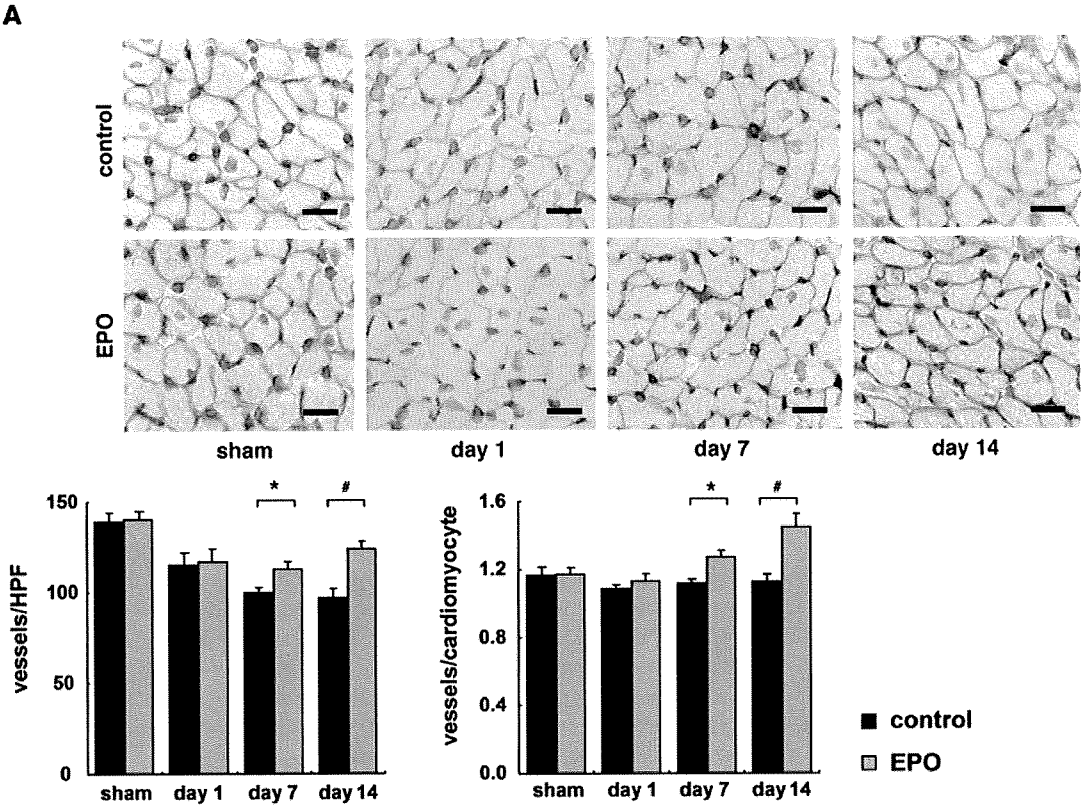
A
control
EPO
sham
day 1
day 7
day 14
vessels/HPF
150
100
50
0
*
#
sham
day 1
day 7
day 14
vessels/cardiomyocyte
1.6
1.2
0.8
0.4
0.0
control
EPO

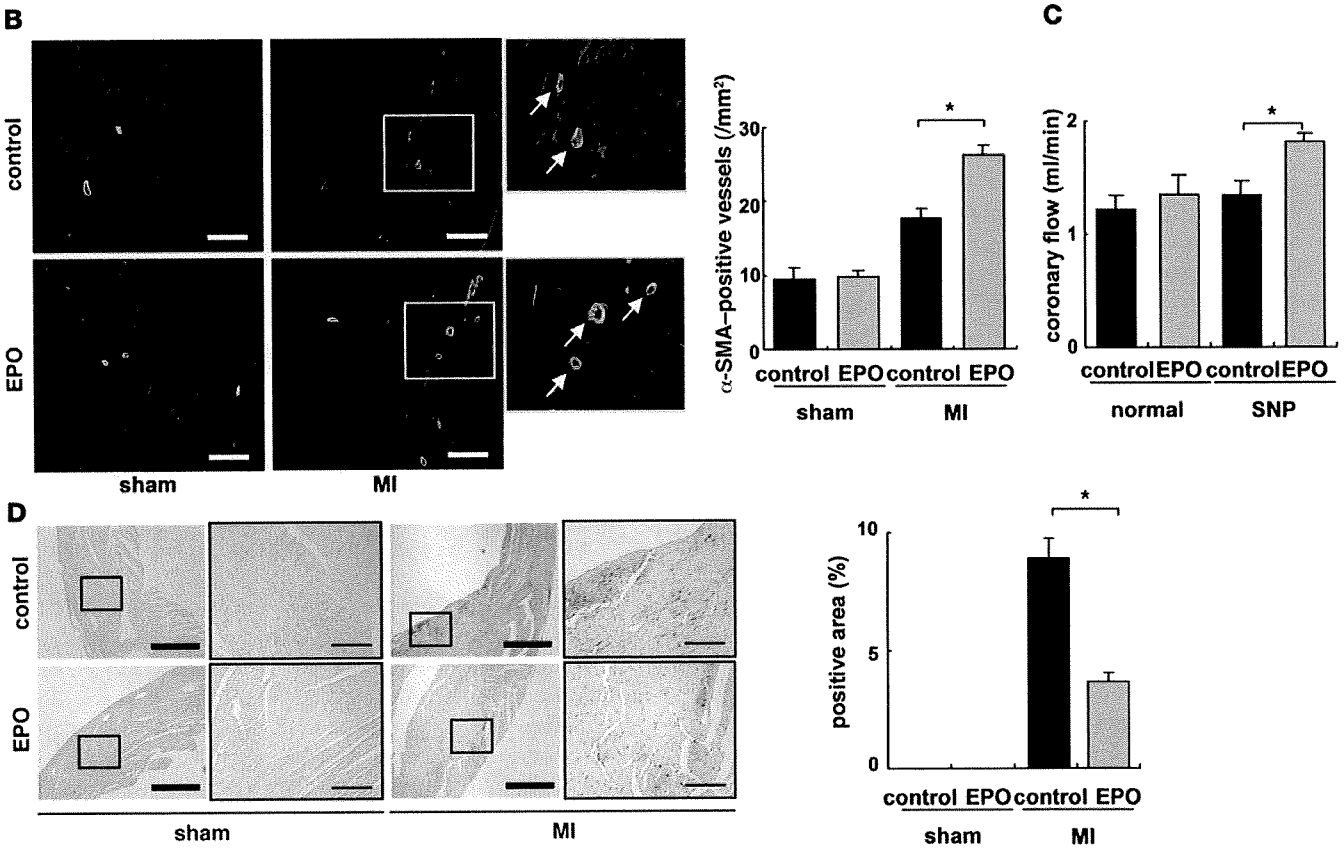
B
control
EPO
sham
MI
α-SMA–positive vessels (/mm²)
30
20
10
0
control EPO control EPO
sham
MI
C
coronary flow (ml/min)
2
1
0
control EPO control EPO
normal
SNP
D
control
EPO
sham
MI
positive area (%)
10
5
0
control EPO control EPO
sham
MI